Progress In Electromagnetics Research M, Vol. 101, 207–218, 2021

Diffraction of the Electromagnetic Plane Waves by Double Half-Plane with Fractional Boundary Conditions

Vasil Tabatadze[1], Kamil Karaçuha[1, *], Eldar Veliev[1, 2], and Ertuğrul Karaçuha[1]

Abstract—In this article, the diffraction of E-polarized electromagnetic plane waves by a double half-plane structure is taken into account. The shift of the upper half-plane through the horizontal axis for different wavenumber and boundary conditions are considered. On the double half-plane structure, fractional boundary conditions are required on the half-plane surfaces. The half-planes are parallel to each other with a variable shift in distance and location. The formulation of the problem is given where the boundary condition is explained, and the integral equations for each half-plane are obtained by using fractional calculus and Fourier Transform techniques. Then, for numerical calculations, the induced current on each half-plane is expressed as the summation of Laguerre polynomials. This leads to having a system of linear algebraic equations needed to be solved. The numerical results show that the shift and the distance between the half-planes give a very important effect on the field values inside and outside the guiding structure. The results are compared and analyzed with Method of Moment and previous results.

1. INTRODUCTION

The diffraction by half-plane is one of the first investigations of the electromagnetic phenomena with the edge condition. The problem keeps its importance because the other geometries such as strip, arc, or wedge are built on the approach developed for the half-plane. The exact solution of the half-plane with a perfect electric conducting surface (PEC) was originally obtained by Sommerfeld [1]. After that, many scientists have contributed to the topic including more complex and different scenarios for the problem including half-planes. Once there exists more than one half-plane in the problem, which may lead to having a guiding structure, and the investigation on the guiding structure is very critical and crucial from the engineering point of view. The analytical outcomes or approximate formula for the physical interpretation is meaningful for not only scientists but also designers and engineers. Our main motivation is to analyze the effect of the variable shift and the distance between the half-planes on the guiding mechanism and total field distribution for different cases of the fractional boundary conditions.

Previously in the literature, there are several comprehensive studies related to diffraction by half-plane including double half-plane, wedge, and half-plane with different medium or boundary conditions [1–13]. Since half-plane geometries have been investigated extensively, it is better to summarize the literature to distinguish previous studies from the present study before the formulation of the problem. In [1, 2], the authors proposed the analytical techniques for the solution of the problem when the source is located inside the guiding structure. Other researchers considered two cases: the diffraction by half-plane aperture and the wedge aperture [3]. Then, in [4], scientists obtained results for the electromagnetic wave scattering when a dielectric object is inserted into the waveguide whereas

Received 20 January 2021, Accepted 11 March 2021, Scheduled 20 March 2021

* Corresponding author: Kamil Karaçuha (karacuha17@itu.edu.tr).

[1] The Informatics Institute of Istanbul Technical University, Istanbul, Turkey. [2] National University of 'Kharkiv Polytechnic Institute', Kharkiv 61000, Ukraine.

a 4-layered material loading is investigated in [5]. Apart from the previous studies, in [5–10], the studies generally focused on the material properties or multiple half-plane geometries.

Formerly, diffraction by a half-plane and wedge geometries with the fractional boundary condition (integral boundary condition) has been examined in [11, 13]. The mathematical formulation and numerical experiments for one half-plane were obtained. After a single half-plane problem, the diffraction by a wedge problem was investigated for different boundary conditions. In these studies, the results are compared with the Method of Moment (MoM) and previous analytical outcomes. The present study can be thought of as the continuation of these researches regarding the fractional boundary condition. However, parallelly located two-half plane (variable shift and distance) with the fractional boundary condition is the novelty of the study.

Recently, the diffraction problems for such canonical structures (half-plane, strip, arc, disc, and wedge) are again the interest of many researchers because the different boundary conditions, material properties, or complex geometries still required to be solved [2, 5–12]. Therefore, problem diversity including boundary conditions, material properties, and excitation types leads the scientist again to target similar geometries. In the consideration, the interaction between two half-planes and waveguiding properties of the structure for different fractional-orders is investigated in the case of the E-polarized plane wave excitation. Previously, similar studies were done by many authors [5–12]. However, all of them use Dirichlet, Neumann, or Impedance boundary conditions. Therefore, the present paper is the first one to employ the fractional boundary conditions for this geometry.

Before going to mathematical manipulation for the diffraction problem, lastly, the fraction calculus employed in electromagnetism and the impedance properties surface with fractional boundary condition are explained briefly. The first studies related to the fractional approach for the electromagnetic theory and its applications are investigated by Engheta [14–18]. Then, Veliyev et al. developed the idea for the boundary condition which is called fractional boundary condition (FBC) [13, 17, 19]. The fractional boundary condition is the generalization of the Dirichlet and Neumann Boundary Conditions. When the fractional-order becomes 0, the boundary condition corresponds to the Dirichlet boundary condition, whereas the Neumann boundary condition is obtained when the fractional order is equal to 1. The fractional boundary condition (i.e., integral boundary condition) used in previous works [19–22] explains a new material property (Perfect Electric Conducting (PEC), Perfect Magnetic Conducting (PMC) or in between). Secondly, there exists a relation between the fractional-order and the impedance value (η) which is $\eta = -i * \tan\left(\frac{\pi}{2}\nu\right)$ for the normal incidence of electromagnetic plane wave [13, 19]. In Fig. 1, the relation between the impedance and the fractional-order (FO) is given. Note that the y-axis of Fig. 1 consists of pure imaginary values.

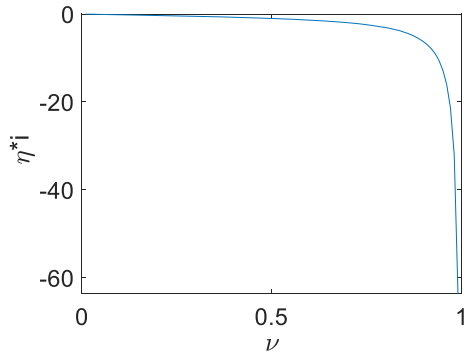

Figure 1. The relation between the impedance and the fractional order.

In the following section, the formulation of the problem and the mathematical manipulations are presented. Then, in Section 3, the numerical analysis of cases such as different values of wavenumber, shift for the upper half-plane, and the angle of incidence is conducted. Later, the comparison with the Method of Moments is presented. Finally, the conclusion is drawn.

2. FORMULATION OF THE PROBLEM

In this section, the geometry of the problem, the derivation of integral equations for each half-plane, obtaining the system of linear algebraic equations by introducing the unknown coefficient, and the orthogonal polynomials are presented. Even though the procedure for the solution of the diffraction problem is quite complex and multi-staged, the approach is straightforward. It is better to summarize the method as follows. First, it is required to express each field component in a mathematical form. Then, the boundary condition is introduced. After that, the coupled-integral equation for each geometry structure is obtained by applying the boundary condition. Later, the main goal is to solve those coupled-integral equations by means of expressing the current density induced on the geometries in terms of complete orthogonal polynomials.

The incidence wave is an E-polarized uniform plane wave as given in Eq. (1). In Fig. 2, the geometry of the problem is shown. The upper plane in general is shifted by the distance a. The distance between half-planes is l.

$$\vec{E}^i(x,y) = \hat{e}_z e^{-ik(x\cos\theta + y\sin\theta)} \tag{1}$$

Here, $\vec{E}^i$ is the incidence wave, $k = 2\pi/\lambda$ the wavenumber, λ the wavelength in free space, θ the angle of incidence, and $\hat{e}_z$ the unit vector in the direction of z. The time dependency is $e^{-i\omega t}$ throughout this paper. The fractional boundary conditions are required on each half-plane surface. Our main goal is to find the scattered field by this structure.

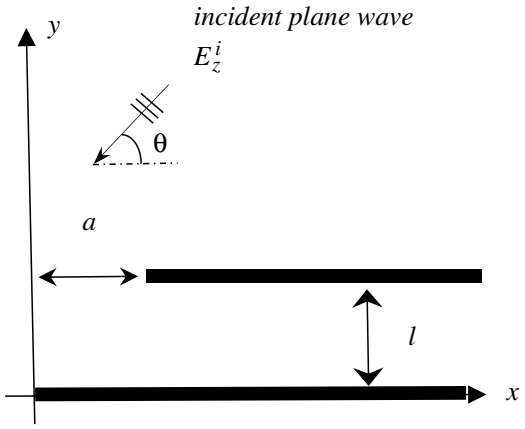

Figure 2. The geometry of the problem.

It is necessary to define the fractional derivative before applying the FBC to the total electric field on the surface of the half-planes. The Riemann-Liouville definition of the fractional derivative for $0 < \nu < 1$ is given as follows [13, 23]:

$$\mathfrak{D}_y^\nu f(y) = \frac{1}{\Gamma(1-\nu)} \frac{d}{dy} \int_{-\infty}^{x} \frac{f(t)\,dt}{(y-t)^\nu} \tag{2}$$

where $0 < \nu < 1$.

Here, $\Gamma(1-\nu)$ is a Gamma function, and the fractional derivative of $f(y)$ is taken with respect to y in the order of ν. After giving the general expression of the fractional derivative, it is better to express the FBC and give a physical interpretation of the boundary condition. The FBC for the lower half-plane is given as:

$$\mathfrak{D}_{ky}^\nu \left(E_z(x,y)\right) = 0, \quad x \in [0,\infty), \quad y = 0 \tag{3}$$

where $E_z(x,y)$ is the total electric field on the surface of the lower half-plane.

Note that the fractional-order derivative is taken concerning ky which is a dimensionless parameter. Keep in mind that y is the normal direction on the surface of the half-plane.

The total electric field $E_z(x,y)$ consists of three major fields. They are the incidence wave $E^i(x,y)$, the scattered electric field due to the lower half-plane $E_z^{s1}(x,y)$, and the scattered field due to the

upper half-plane $E_z^{s2}(x,y)$. The scattered field can be found by the convolution of the fractional Green function G^ν and the induced fractional current densities (f_1^ν and f_2^ν) for each half-plane, respectively as [13, 17, 19]:

$$E_z(x,y) = E_z^{s1}(x,y) + E_z^{s2}(x,y) + E_z^i(x,y) \tag{4}$$

Here,

$$E_z^{s1}(x,y) = \int_0^\infty f_1^\nu\left(x'\right) G^\nu\left(x-x', y\right) dx',$$

$$E_z^{s2}(x,y) = \int_a^\infty f_2^\nu\left(x'\right) G^\nu\left(x-x', y-l\right) dx'.$$

where $G^\nu(x-x', y-y') = -\frac{i}{4}\mathfrak{D}_{ky}^\nu H_0^{(1)}(k\sqrt{(x-x')^2+(y-y')^2}\,)$.

To apply FBC, the representation of the Hankel's function as the superposition of plane waves is preferred [13, 24]. The main purpose of this fact is that the fractional derivative of the exponential terms is easy to implement as $\mathfrak{D}_x^\nu(e^{ikx}) = (ik)^\nu e^{ikx}$ [22, 23]. Then, the Hankel function is expressed as:

$$H_0^{(1)}\left(k\sqrt{(x-x')^2+(y-y')^2}\right) = \frac{1}{\pi}\int_{-\infty}^{\infty} e^{ik\left[(x-x')q+|y-y'|\sqrt{1-q^2}\right]}\frac{dq}{\sqrt{1-q^2}}.$$

To find the scattered electric field of each half-plane, Eq. (4) is used and put into Eq. (3). Then, Eq. (5) is obtained for the lower half-plane.

$$-\frac{i}{4\pi}e^{\pm i\pi\nu}\left(\begin{array}{l}\displaystyle\int_{-\infty}^{\infty} F_1^\nu(q)\, e^{ikxq}\left(1-q^2\right)^{\nu-\frac{1}{2}} dq \\ \displaystyle+\int_{-\infty}^{\infty} F_2^\nu(q)\, e^{ik\left[xq+l\sqrt{1-q^2}\right]}\left(1-q^2\right)^{\nu-\frac{1}{2}} dq\end{array}\right) + (-i\sin\theta)^\nu\, e^{-ikx\cos\theta} = 0 \tag{5}$$

for $x \in [0,\infty)$ and $y = 0$.

$$F_1^\nu(q) = \int_0^\infty f_1^\nu\left(x'\right) e^{-ikqx'} dx' F_2^\nu(q) = \int_a^\infty f_2^\nu\left(x'\right) e^{-ikqx'} dx' \tag{6}$$

Eq. (6) is the Fourier transform of the fractional current densities given in Eq. (4). Note that the current densities (f_1^ν and f_2^ν) have only non-zero values on the corresponding surfaces. Obtaining Eq. (5) is an important step of the study. This is the integral equation for the lower half-plane. The main purpose is to solve the integral equations obtained from the boundary condition satisfaction for each half-plane. With the same approach, the boundary condition on the upper half-plane will have the form as Eq. (7).

$$\mathfrak{D}_{ky}^\nu\left(E_z(x,y)\right) = 0, \;\; x \in [a,\infty), \;\; y = l \tag{7}$$

Analogically, for the upper half-plane, the integral equation will be as:

$$-\frac{i}{4\pi}e^{\pm i\pi\nu}\left(\begin{array}{l}\displaystyle\int_{-\infty}^{\infty} F_1^\nu(q)\, e^{ik\left[xq+l\sqrt{1-q^2}\right]}\left(1-q^2\right)^{\nu-\frac{1}{2}} dq \\ \displaystyle+\int_{-\infty}^{\infty} F_2^\nu(q)\, e^{ikxq}\left(1-q^2\right)^{\nu-\frac{1}{2}} dq\end{array}\right) + (-i\sin\theta)^\nu\, e^{-ik(x\cos\theta+l\sin\theta)} = 0 \tag{8}$$

for $x \in [a,\infty)$ and $y = l$.

Let's introduce $\xi = x - a$, $x = (\xi + a)$ for Eq. (8). Then, the equation becomes:

$$\frac{i}{4\pi} e^{\pm i\pi\nu} \left(\begin{array}{l} \int\limits_{-\infty}^{\infty} e^{ikqa} F_1^{\nu}(q) e^{ik\left[(\xi)q + l\sqrt{1-q^2}\right]} \left(1-q^2\right)^{\nu-\frac{1}{2}} dq \\ + \int\limits_{-\infty}^{\infty} e^{ikqa} F_2^{\nu}(q) e^{ik(\xi)q} \left(1-q^2\right)^{\nu-\frac{1}{2}} dq \end{array} \right) = (-i\sin\theta)^{\nu} e^{-ik\cos\theta a} e^{-ik((\xi)\cos\theta + l\sin\theta)} \quad (9)$$

For further manipulations, the change of dummy variable is also employed for Eq. (6) as $\tilde{x} = x' - a$, $x' = \tilde{x} + a$, and the procedure is given as:

$$F_2^{\nu}(q) = \int\limits_0^{\infty} f_2^{\nu}(\tilde{x}+a) e^{-ikq(\tilde{x}+a)} d\tilde{x} = e^{-ikqa} \int\limits_0^{\infty} f_2^{\nu}(\tilde{x}+a) e^{-ikq\tilde{x}} d\tilde{x} = e^{-ikqa} \int\limits_0^{\infty} \tilde{f}_2^{\nu}(\tilde{x}) e^{-ikq\tilde{x}} d\tilde{x} \quad (10)$$

where $f_2^{\nu}(\tilde{x}+a) = \tilde{f}_2^{\nu}(\tilde{x})$.

After this point, the coupled integral equations are obtained. Then, the solution of these integral equations is aimed. To solve these integral equations (Eqs. (5) and (9)), the approach is as follows:

The current densities on each corresponding half-plane are expressed as the summation of the Laguerre polynomials by taking into account the edge conditions. The reason for choosing the Laguerre polynomials is that these polynomials are defined between $[0, \infty)$ which is suitable for the geometry of the problem. For instance, Gegenbauer or Chebyshev polynomials are preferred in the case of strip problems.

To solve Eqs. (5) and (9), the fractional current densities are expressed as the summation of the Laguerre polynomials with the corresponding weight function. The weight function is chosen so that the edge condition is satisfied [19, 24, 25]. In Eq. (11), the expansion of the induced fractional current density f_1^{ν} on the lower half-plane is given. Note that $\mathbf{f}_n^1$ are the unknown coefficient that needs to be found by using Eqs. (5) and (9).

$$f_1^{\nu}\left(\frac{\varsigma}{k}\right) = e^{-\varsigma}\varsigma^{\nu-\frac{1}{2}} \sum_{n=0}^{\infty} \mathbf{f}_n^1 L_n^{\nu-\frac{1}{2}}(2\varsigma), \quad \varsigma = kx \quad (11)$$

The Fourier transform of Eq. (11) is given as [12]:

$$F_1^{\nu}(q) = \int\limits_0^{\infty} f_1^{\nu}\left(x'\right) e^{-ikqx'} dx' = \frac{1}{k} \sum_{n=0}^{\infty} \mathbf{f}_n^1 \gamma_n^{\nu} D_n^{\nu}(q) \quad (12)$$

where $\gamma_n^{\nu} = \frac{\Gamma(n+\nu+\frac{1}{2})}{\Gamma(n+1)}$, $D_n^{\nu}(q) = \frac{(iq-1)^n}{(iq+1)^{\nu+n+\frac{1}{2}}}$.

Also for the upper half-plane, the induced fractional current density f_2^{ν} on the upper half-plane and its Fourier transform are given, respectively as:

$$f_2^{\nu}\left(\frac{\varsigma}{k}\right) = e^{-\varsigma}\varsigma^{\nu-\frac{1}{2}} \sum_{n=0}^{\infty} \mathbf{f}_n^2 L_n^{\nu-\frac{1}{2}}(2\varsigma), \quad \varsigma = kx \quad (13)$$

Here,

$$F_2^{\nu}(q) = e^{-ikqa} \int\limits_0^{\infty} \tilde{f}_2^{\nu}\left(x'\right) e^{-ikqx'} dx' = \frac{e^{-ikqa}}{k} \sum_{n=0}^{\infty} \mathbf{f}_n^2 \gamma_n^{\nu} D_n^{\nu}(q) \quad (14)$$

Putting Eqs. (12) and (14) into Eq. (5), then the first integral equation for the lower half-space will be:

$$\mathbf{I_3} = \mathbf{I_1} + \mathbf{I_2} \quad (15)$$

where,

$$\mathbf{I_1} = \chi \int\limits_{-\infty}^{\infty} \sum_{n=0}^{\infty} \mathbf{f}_n^1 \gamma_n^{\nu} D_n^{\nu}(q) e^{ikxq} \left(1-q^2\right)^{\nu-\frac{1}{2}} dq$$

$$\mathbf{I_2} = \chi \int_{-\infty}^{\infty} \sum_{n=0}^{\infty} \mathbf{f}_n^2 \gamma_n^{\nu} D_n^{\nu}(q)\, \rho e^{ik\left(xq+l\sqrt{1-q^2}\right)} \left(1-q^2\right)^{\nu-\frac{1}{2}} dq$$

$$\mathbf{I_3} = (-i\sin\theta)^{\nu} e^{-ikx\cos\theta}$$

Here, $\chi = -\frac{i}{4\pi k}\, e^{\pm i\pi\nu}$ and $\rho = e^{-ikqa}$.

To solve the integral equation given in Eq. (15), some steps need to be followed. Note that the main aim is to obtain unknown coefficients $\mathbf{f}_n^1$ and $\mathbf{f}_n^2$. After that, the current densities, then, the field distribution can be found.

First, multiplying both sides of Eq. (15) by $e^{-\varsigma}\varsigma^{\nu-\frac{1}{2}} L_n^{\nu-\frac{1}{2}}(2\varsigma)$ to employ orthogonality. Then, it is required to take an integral with respect to x in the interval of $[0,\infty)$, and finally, it is needed to use the property [11, 13, 24] given as:

$$\int_0^{\infty} x^{\lambda} e^{-px} L_n^{\lambda}(cx)\, dx = \frac{\Gamma(\lambda+n+1)(p-c)^n}{\Gamma(n+1)p^{\lambda+n+1}}.$$

Finally, the System of Linear Algebraic Equations (SLAE) for the lower half-plane is obtained as:

$$\sum_{n=0}^{\infty} \mathbf{f}_n^1 \gamma_n^{\nu} C_{nm}^{11} (-1)^{n+m} + \sum_{n=0}^{\infty} \mathbf{f}_n^2 \gamma_n^{\nu} C_{nm}^{12} (-1)^{n+m} = -4\pi k e^{i\frac{\pi}{2}(1-3\nu)} (\sin\theta)^{\nu} D_n^{\nu}(\cos\theta) \tag{16}$$

The same procedure is applied to Eq. (9), and the SLAE for the upper half-plane is obtained as:

$$\begin{aligned} &\sum_{n=0}^{\infty} \mathbf{f}_n^1 \gamma_n^{\nu} C_{nm}^{21} (-1)^{n+m} + \sum_{n=0}^{\infty} \mathbf{f}_n^2 \gamma_n^{\nu} C_{nm}^{22} (-1)^{n+m} \\ &= -4\pi k e^{i\frac{\pi}{2}(1-3\nu)} (\sin\theta)^{\nu} D_n^{\nu}(\cos\theta)\, e^{-ikl\sin\theta} e^{-ika\cos\theta} \end{aligned} \tag{17}$$

Here,

$$C_{nm}^{i,i} = \int_{-\infty}^{\infty} \left(1-q^2\right)^{\nu-\frac{1}{2}} \frac{(1-iq)^{n-m-\nu-\frac{1}{2}}}{(1+iq)^{n-m+\nu+\frac{1}{2}}}\, dq, \quad i=1,2,$$

$$C_{nm}^{i,j} = \int_{-\infty}^{\infty} \Lambda(q) \left(1-q^2\right)^{\nu-\frac{1}{2}} \frac{(1-iq)^{n-m-\nu-\frac{1}{2}}}{(1+iq)^{n-m+\nu+\frac{1}{2}}}\, dq, \quad i,j=1,2, \quad i\neq j,$$

and

$$\gamma_n^{\nu} = \frac{\Gamma(n+\nu+\frac{1}{2})}{\Gamma(n+1)}, \quad D_n^{\nu}(q) = \frac{(iq-1)^n}{(iq+1)^{\nu+n+\frac{1}{2}}}.$$

Note that $\Lambda(q) = e^{\pm ikqa} e^{ikl\sqrt{1-q^2}}$, and in Eqs. (16) and (17), (+) sign is for $i=1$ and (−) sign for $i=2$.

The final expressions for the scattered electric field due to the lower and upper half-planes are respectively as:

$$E_z^{s1} = \int_{-\infty}^{\infty} \chi F_1^{\nu}(q) e^{ik\left(xq+|y|\sqrt{1-q^2}\right)} (1-q^2)^{\frac{\nu-1}{2}} dq \quad (+ \text{ for } y>l \;-\; \text{for } y<l) \tag{18}$$

$$E_z^{s2} = \int_{-\infty}^{\infty} \chi F_2^{\nu}(q)\, e^{ik\left(xq+|y-l|\sqrt{1-q^2}\right)} \left(1-q^2\right)^{\frac{\nu-1}{2}} dq \quad (+ \text{ for } y>0 \;-\; \text{for } y<0) \tag{19}$$

where $\chi = -\frac{i}{4\pi k}\, e^{\pm i\pi\nu}$.

3. NUMERICAL RESULTS

In this part, the numerical results for several cases are presented. Different values of the electrical length (kl) among the half-planes, incidence angle, and fractional order (ν) are investigated, and the near electric field distributions are given. The results are compared with the previous studies and Method of Moments (MoM) [1, 26–28]. Based on the mathematical algorithms given in the theoretical part, the program package was created in MatLab. The comparison method is chosen as MoM because the approach for the solution of the integral equation is similar. In other words, the main purpose is to express the current density on the scatterer in terms of predefined bases and converting integral equations into SLAE by employing the inner product and orthogonality [27, 28]. For the Method of Moment approach, the sub-domain basis function is chosen as a piecewise constant pulse function. For the test function, a point matching approach is chosen.

Before presenting the experimental results, it is better to highlight the verification. First, we consider the case when the fractional order $\nu = 0.01$ which corresponds to the perfect electric conductor (PEC). This is a classical case known in literature [1, 2]. The results coincide with the previous study. Also, the study is compared with the plane wave diffraction by a half-plane [11]. Note that the study [11] is also obtained by the Fractional Derivative Method. To compare the studies, the shift parameter a, distance parameter l and k (wavenumber) are taken as 0, 0.001, and π, respectively (Note that $k \gg l$). The result coincides with any fractional order. After denoting the verification of the study obtained here with the previous studies as [1] and the half-plane problem satisfying the FBC, it is better to explain the figures.

Figure 3 shows the near field distribution for cases $\nu = 0.01$ and $a = 0.0001$ at different frequencies. Fig. 3(a) corresponds to the normal incidence case for $= \pi$. Note that between the half-planes, we see the standing waves. Fig. 3(b) corresponds to similar parameters. Note that only the incident angle is

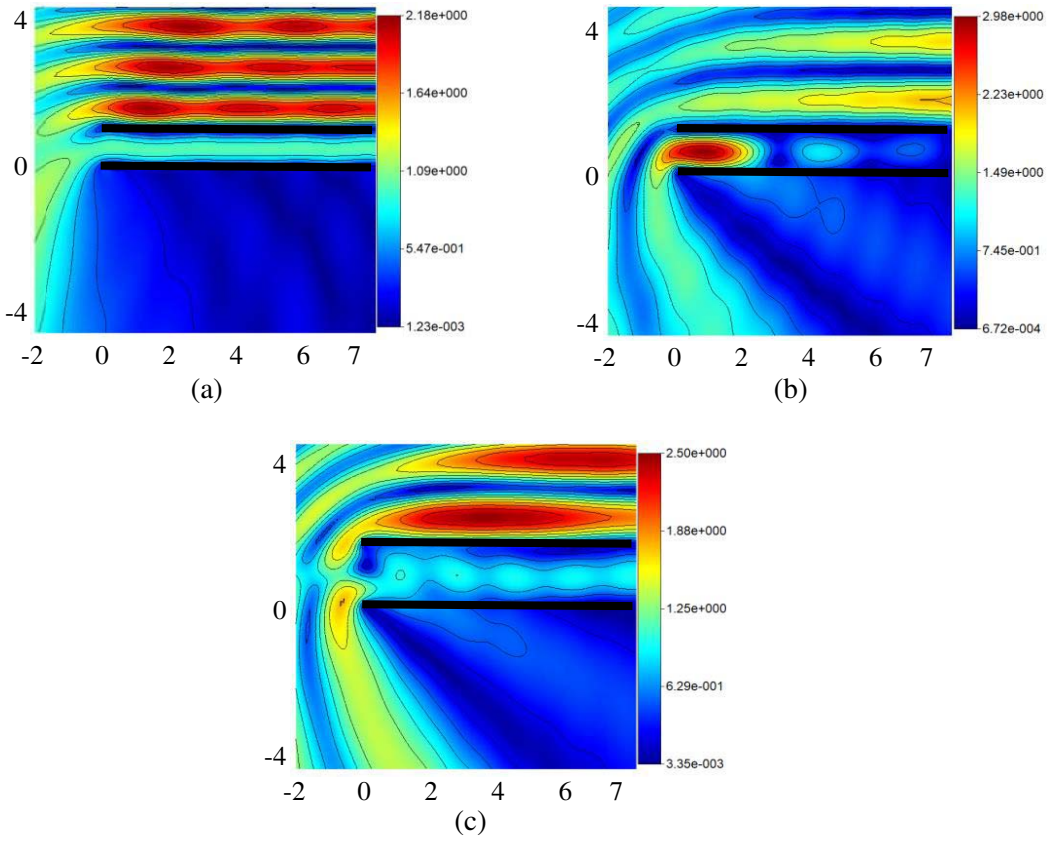

Figure 3. The total near field distribution (for animation, see [26]). (a) $\nu = 0.01$, $kl = \pi$, $\theta = \frac{\pi}{2}$, (b) $\nu = 0.01$, $kl = \pi$, $\theta = \frac{3\pi}{4}$, (c) $\nu = 0.01$, $kl = \frac{3\pi}{2}$, $\theta = \frac{3\pi}{4}$.

different. As we see, some parts of the energy penetrate inside but cannot propagate at a far distance. Fig. 3(c) shows the case when the electrical length between half-planes is $kl = \frac{3\pi}{2}$. In this case, we have a propagating wave inside the structure. Here, the half-planes behave like a waveguide, and there exist cut-off frequencies for different modes [27].

After that, we consider the case when $\nu = 1$, and it corresponds to the perfect magnetic conductor (PMC). Fig. 4 shows the near field distribution and Poynting vector distribution for the normal incidence when $kl = \pi$ [27]. As shown in the figures, the traveling wave is formed inside the structure, and it propagates by reflecting plates. This case is also a classical case. After presenting the well-known two cases, it is better to investigate the half-planes satisfying the fractional boundary condition with a non-integer order between 0 and 1.

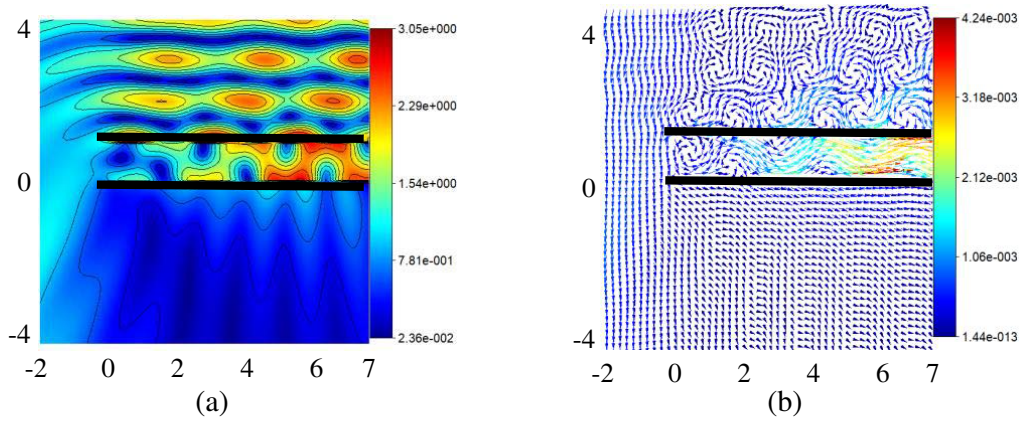

Figure 4. Total near electric field (a) and Poynting vector distribution (b) at the parameters $\nu = 1$, $kl = \pi$, $\theta = \frac{\pi}{2}$ (for animation see [26]).

Next, we consider the case when the fractional order $\nu = 0.5$. The corresponding impedance value $\eta = -i$ [19, 20]. Fig. 5(a) shows the normal incidence case. Inside the structure, we have a standing wave. Fig. 5(b) shows the same scenario for the incidence angle $\theta = \frac{3\pi}{4}$. Inside the structure, there is a traveling wave whose amplitude is higher than outside the structure. Note that this is different from the case considered for the perfect electric and perfect magnetic conductor cases.

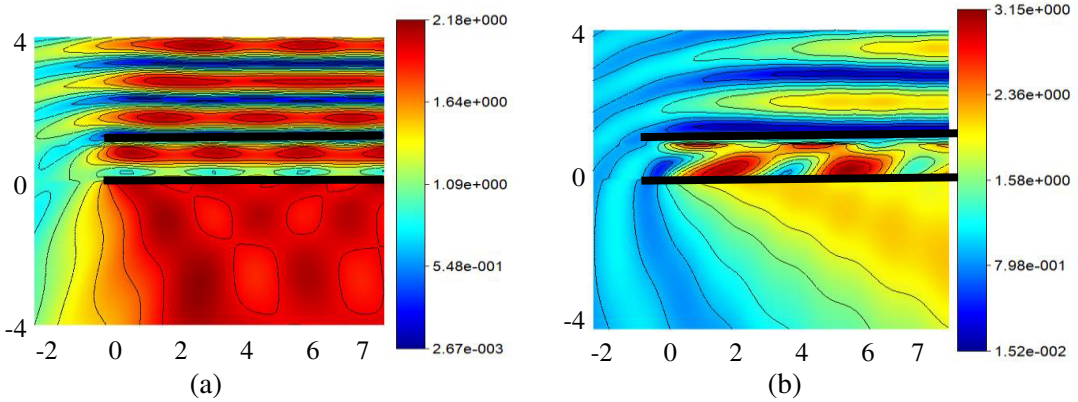

Figure 5. Total near field distribution (for animation see [26]). (a) $\nu = 0.5$, $kl = \pi$, $\theta = \frac{\pi}{2}$, (b) $\nu = 0.5$, $kl = \pi$, $\theta = \frac{3\pi}{4}$.

We have also considered the cases when $\nu = 0.75$ and $\nu = 0.25$. The results are given in Fig. 6. As can be seen, again the electric field inside the structure has a higher amplitude than the outside. Also, the structure of the traveling wave is different from classical cases.

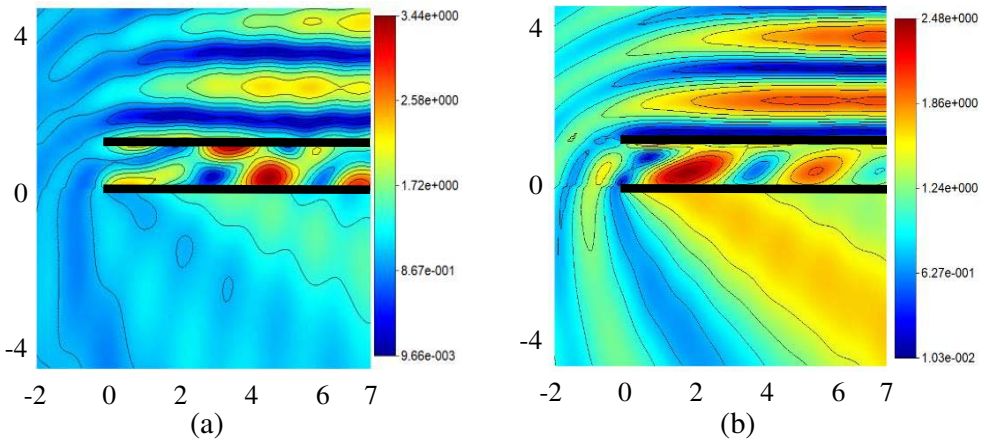

Figure 6. Total near field distribution (for animation see [26]). (a) $\nu = 0.75$, $kl = \pi$, $\theta = \frac{3\pi}{4}$, (b) $\nu = 0.25$, $kl = \pi$, $\theta = \frac{3\pi}{4}$.

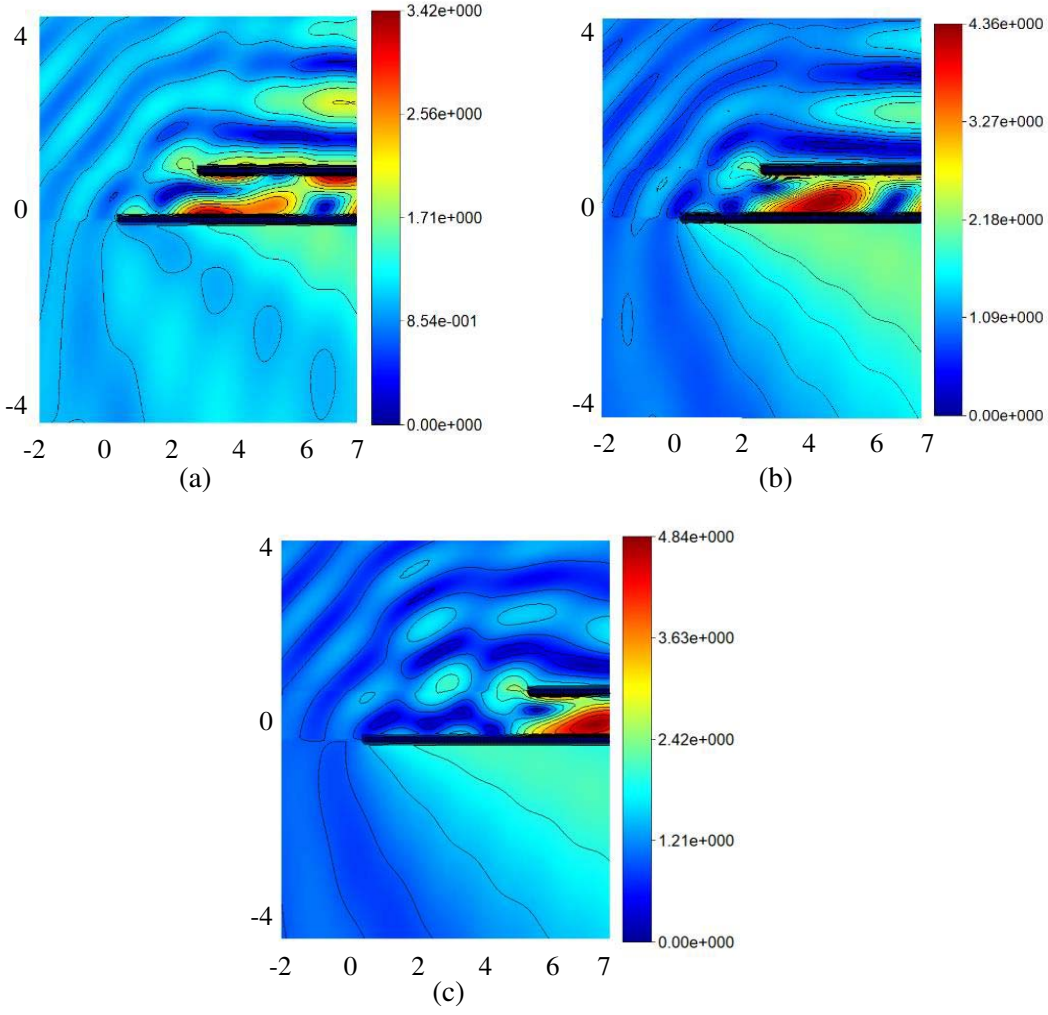

Figure 7. Total near field distribution (for animation see [23]). (a) $\nu = 0.5$, $kl = \pi$, $\theta = \frac{3\pi}{4}$, $a = 10$, (b) $\nu = 0.5$, $kl = \pi$, $\theta = \frac{3\pi}{4}$, $a = 20$, (c) $\nu = 0.75$, $kl = \pi$, $\theta = \frac{3\pi}{4}$, $a = 10$.

In all previous cases, the length of the half-planes was the same and not shifted ($a = 0.001$). Next, we consider the cases when $a \neq 0$. Fig. 7 shows the near field distribution for this case. In the case of Fig. 7(a), $\nu = 0.5$ case is considered when the upper half-plane is shifted by $a = 10$. As we can see, the amplitude of the field inside the structure is higher than outside as it was in the case of Fig. 5(b). However, the contrast is higher here (4.36 vs 3.15). This can be explained by the fact that the electric field easily penetrates inside because the incident field is reflected from the lower half-plane and then, is reflected inside the waveguide. The contrast becomes even higher when we take $a = 20$. Then, the maximum field value becomes 4.84. Fig. 7(c) shows the case when $\nu = 0.75$. If we compare this final result with Fig. 6(a) case, the structure of the field distribution changes, but the high field value is practically the same.

All the field animations related to the results given in this article are uploaded to YouTube and can be found at the link [26].

The FBC is the generalization of the well-known Dirichlet and Neumann boundary conditions. Once the problem is solved for arbitrary fractional-order ν between 0 and 1 (i.e., the integral equations are obtained for variable ν as it is done in the Formulation of the Problem Section), the numerical experiments can be done for different fractional orders. It would be wise to summarize the section at that point before passing through the comparison of the method with MoM. In this section, first, the previous studies [1, 11] are highlighted, and at the limit case ($l = 0.001$), the results coincide. After that, the numerical results are given for several scenarios.

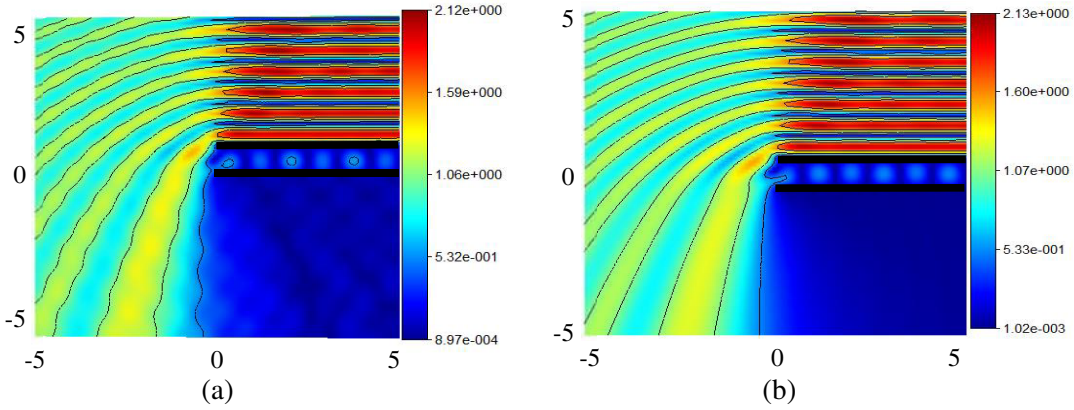

Figure 8. Comparison of total near field distributions with fractional method and method of moments for $kl = \frac{3\pi}{2}$, $\theta = \frac{\pi}{2}$, $a = 0.0001$, (a) fractional method ($\nu = 0.01$), (b) method of moments.

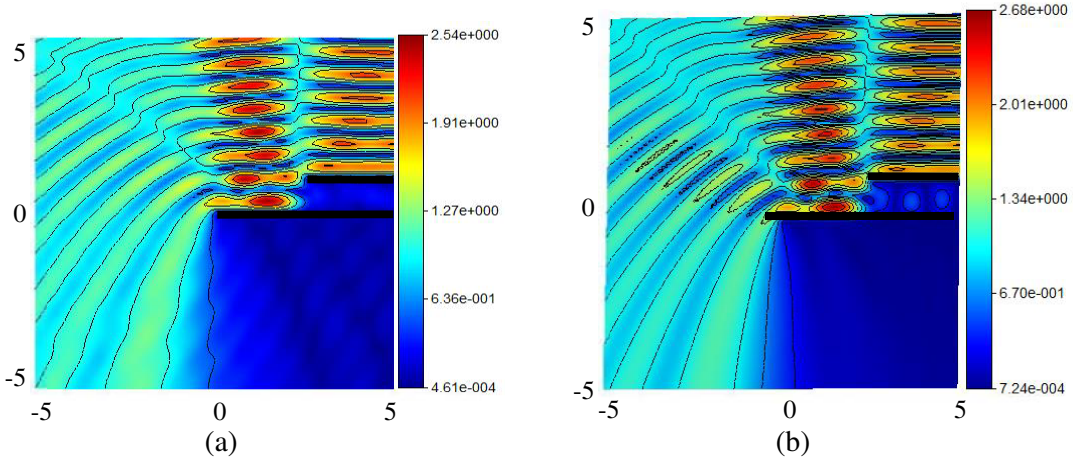

Figure 9. Comparison of total near field distributions with fractional method and method of moment for $kl = \frac{3\pi}{2}$, $\theta = \frac{\pi}{2}$, $a = 2.5$, (a) fractional method ($\nu = 0.01$), (b) method of moments.

Now, in Fig. 8, the comparison is done between the fractional derivative method and MoM with given parameters. In that figure, there is approximately no shift between the half-planes. As you can see, the distributions obtained by the two methods give approximately the same results.

In Fig. 9, again, the comparison of two methods for the near electric field distribution is given. In that case, there exists a shift (a) between two half-planes. Also, the results are approximately the same.

4. CONCLUSION

In this study, the diffraction problem solution of the electromagnetic waves by a double half-plane structure is considered. The integral boundary condition is satisfied on each half-plane surface. The boundary condition is the generalization of the Dirichlet and Neumann boundary conditions. Once, we solve the integral equation satisfying the integral boundary condition (fractional boundary condition), for different values of the fractional order, the required information such as field distributions, Poynting vector distribution, and current densities can be obtained. In this study, the theoretical part is given, and based on it, the numerical experiments are realized. There are investigated classical cases of the PEC and PMC, and they are compared to the intermediate cases of the fractional order. The comparison is highlighted with previous studies. The traveling wave with the higher amplitude is observed inside the half-planes for the intermediate fractional order, in comparison with the PEC and PMC cases. Also, the differences between two-half planes and shifted two-half-planes are investigated, and the differences are revealed. Then, the comparison is done with MoM. The results are found approximately the same. The main advantage of the fractional derivative approach is that once the integral equations are obtained, only the numerical part is repeated for different fractional orders. Therefore, the formulation of the problem, obtaining the integral equations for each half-plane, and converting integral equations into SLAE are provided in the most general form. Then, for different boundary conditions, only numerical analysis is performed whereas the other methods require, again, the formulation of the problem for each boundary condition.

ACKNOWLEDGMENT

The authors of the paper would like to thank the National Center for High-Performance Computing (UHEM) located at Istanbul Technical University for utilization and access.

REFERENCES

1. Mittra, R. and S. W. Lee, *Analytical Technique in the Theory of Guided Waves*, The Macmillan Company, 1971.
2. Nethercote, M. A., R. C. Assier, and I. D. Abrahams, "Analytical methods for perfect wedge diffraction: A review," *Wave Motion*, Vol. 93, 102479, 2020.
3. Rudduck, R. and L. Tsai, "Aperture reflection coefficient of TEM and TE01 mode parallel-plate waveguides," *IEEE Transactions on Antennas and Propagation*, Vol. 16, No. 1, 83–89, 1968.
4. Hame, Y. and I. H. Tayyar, "Plane wave diffraction by dielectric loaded thick-walled parallel-plate impedance waveguide," *Progress In Electromagnetics Research*, Vol. 44, 143–167, 2004.
5. Zheng, J.-P. and K. Kobayashi, "Plane wave diffraction by a finite parallel-plate waveguide with four-layer material loading: Part 1 — The case of E-polarization," *Progress In Electromagnetics Research B*, Vol. 6, 1–36, 2008.
6. Alkumru, A., "Plane wave diffraction by three parallel thick impedance half-planes," *Journal of Electromagnetic Waves and Applications*, Vol. 12, No. 6, 801–819, 1998.
7. Tiberio, R. and R. Kouyoumjian, "Calculation of the high-frequency diffraction by two nearby edges illuminated at grazing incidence," *IEEE Transactions on Antennas and Propagation*, Vol. 32, No. 11, 1186–1196, 1984.
8. Umul, Y. Z., "Diffraction of waves by a boundary between two half-planes with different resistivities," *Optics Letters*, Vol. 40, No. 7, 1306–1309, 2015.

9. Umul, Y. Z., "Wave diffraction by a reflectionless half-plane," *Applied Optics*, Vol. 56, No. 33, 9293–9300, 2017.
10. Basdemir, H. D., "Scattering of plane waves by a rational half-plane between DNG media," *Optik*, Vol. 179, 47–53, 2019.
11. Veliyev, E. I., V. Tabatadze, K. Karaçuha, and E. Karaçuha, "The diffraction by the half-plane with the Fractional boundary condition," *Progress In Electromagnetics Research M*, Vol. 88, 101–110, 2020.
12. Tabatadze, V., K. Karaçuha, E. I. Veliyev, and E. Karaçuha, "The diffraction by two half-planes and wedge with the fractional boundary condition," *Progress In Electromagnetics Research M*, Vol. 91, 1–10, 2020.
13. Veliev, E. I., T. Ahmedov, and M. Ivakhnychenko, *Fractional Operators Approach and Fractional Boundary Conditions*, *Electromagnetic Waves*, Vitaliy Zhurbenko (ed.), IntechOpen, 2011, doi: 10.5772/16300.
14. Engheta, N., "Use of fractional integration to propose some"fractional" solutions for the scalar Helmholtz equation," *Progress In Electromagnetics Research*, Vol. 12, 107–132, 1996.
15. Engheta, N., "Fractional curl operator in electromagnetics," *Microwave and Optical Technology Letters*, Vol. 17, No. 2, 86–91, 1998.
16. Engheta, N., "On fractional calculus and fractional multipoles in electromagnetism," *IEEE Transactions on Antennas and Propagation*, Vol. 44, No. 4, 554–566, 1996.
17. Veliev, E. I. and N. Engheta, "Generalization of Green's theorem with fractional differintegration," *Proceedings of IEEE AP-S International Symposium & USNC/URSI National Radio Science Meeting*, 2003.
18. Engheta, N., "Fractionalization methods and their applications to radiation and scattering problems," *Proceedings of International Conference on Mathematical Methods in Electromagnetic Theory*, 34–40, 2000.
19. Ivakhnychenko, M., E. Veliev, and T. Ahmedov, "Scattering properties of the strip with fractional boundary conditions and comparison with the impedance strip," *Progress In Electromagnetics Research C*, Vol. 2, 189–205, 2008.
20. Karaçuha, K., E. I. Veliyev, V. Tabatadze, and E. Karaçuha, "Application of the method of fractional derivatives to the solution of the problem of plane wave diffraction by two axisymmetric strips of different sizes," *Proceedings of URSI International Symposium on Electromagnetic Theory (EMTS)*, San Diego, USA, 2019.
21. Tabatadze, V., K. Karaçuha, and E. I. Veliev, "The fractional derivative approach for the diffraction problems: Plane wave diffraction by two strips with the fractional boundary conditions," *Progress In Electromagnetics Research C*, Vol. 95, 251–264, 2019.
22. Karaçuha, K., E. I. Veliyev, V. Tabatadze, and E. Karaçuha, "Analysis of current distributions and radar cross sections of line source scattering from impedance strip by fractional derivative method," *Advanced Electromagnetics*, Vol. 8, No. 2, 108–113, 2019.
23. Podlubny, I., *Fractional Differential Equations: An Introduction to Fractional Derivatives, Fractional Differential Equations, to Methods of Their Solution and Some of Their Applications*, Elsevier, 1998.
24. Prudnikov, H. P., Y. H. Brychkov, and O. I. Marichev, *Special Functions, Integrals and Series*, Vol. 2, Gordon and Breach Science Publishers, 1986.
25. Meixner, J., "The behavior of electromagnetic fields at edges," *IEEE Transactions on Antennas and Propagation*, Vol. 20, No. 4, 442–446, 1972.
26. YouTube. [Online]. Available: https://www.youtube.com/user/vasilitabatadze/playlists. [Accessed: 15-Jan-2021].
27. Balanis, C. A., *Antenna Theory Analysis and Design*, Wiley, Hoboken, NJ, 2016.
28. Karaçuha, K., V. Tabatadze, and E. I. Veliev, "Plane wave diffraction by the strip with an integral boundary condition," *Turkish Journal of Electrical Engineering & Computer Sciences*, Vol. 28, No. 3, 1776–1790, 2020, doi: 10.3906/elk-1906-170.